Changes in snow cover over China in the 21st century as simulated by a high resolution regional climate model

Changes in snow cover over China in the 21st century as simulated by a high resolution regional climate model

Ying Shi[1], Xuejie Gao[1,3], Jia Wu[1] and Filippo Giorgi[2]

[1] National Climate Center, China Meteorological Administration, Beijing 100081,
People's Republic of China
[2] The Abdus Salam International Centre for Theoretical Physics, Trieste 34100, Italy

E-mail: gaoxj@cma.gov.cn

Abstract
On the basis of the climate change simulations conducted using a high resolution regional
climate model, the Abdus Salam International Centre for Theoretical Physics (ICTP) Regional
Climate Model, RegCM3, at 25 km grid spacing, future changes in snow cover over China are
analyzed. The simulations are carried out for the period of 1951–2100 following the IPCC
SRES A1B emission scenario. The results suggest good performances of the model in
simulating the number of snow cover days and the snow cover depth, as well as the starting and
ending dates of snow cover to the present day (1981–2000). Their spatial distributions and
amounts show fair consistency between the simulation and observation, although with some
discrepancies. In general, decreases in the number of snow cover days and the snow cover
depth, together with postponed snow starting dates and advanced snow ending dates, are
simulated for the future, except in some places where the opposite appears. The most dramatic
changes are found over the Tibetan Plateau among the three major snow cover areas of
Northeast, Northwest and the Tibetan Plateau in China.

Keywords: climate change, regional climate model, snow cover

1. Introduction

The cryosphere, atmosphere, hydrosphere, land surface and
biosphere are the five major physical components of the
climate system. As part of the cryosphere, snow cover derives
its importance to atmospheric thermal and dynamical processes
from its high reflectivity (albedo) for short-wave solar radiation
and consequent effect on the surface energy budget and the
Earth's radiative balance. In China, deep snow cover is one
of the major weather and climate disasters in the cold seasons,
which causes loss of human life and disruption of the economy
each year. By burying the fodder grass, the thick snow
cover may lead to the loss of grassland animal husbandry and
the death of wild animals in Inner Mongolia (located in the

northern border areas extending from the eastern part of the
sub-region NW to the eastern part of the sub-region NE in
figure 1(a)) and western China. Meanwhile, snow cover in
winter is beneficial to agriculture by conserving the heat of the
surface and thus protecting crops (mainly winter wheat) from
the cold air, and by providing water to the crops in the dry
spring following. In addition, snow cover over the mountains
provides most of the stream flow runoff in Northwest China
(NW), an area with a prevalence of arid and semi-arid climate.
Important influences of snow cover on local and regional
climate have also been widely reported in China (see e.g. Chen
2001).

While snow cover shows strong seasonal and interannual
variations, significant decreases of it are found in most regions
in the world due to the observed warming in recent decades,
primarily in spring and thus following into summer, but not

---

[3] Author to whom any correspondence should be addressed.
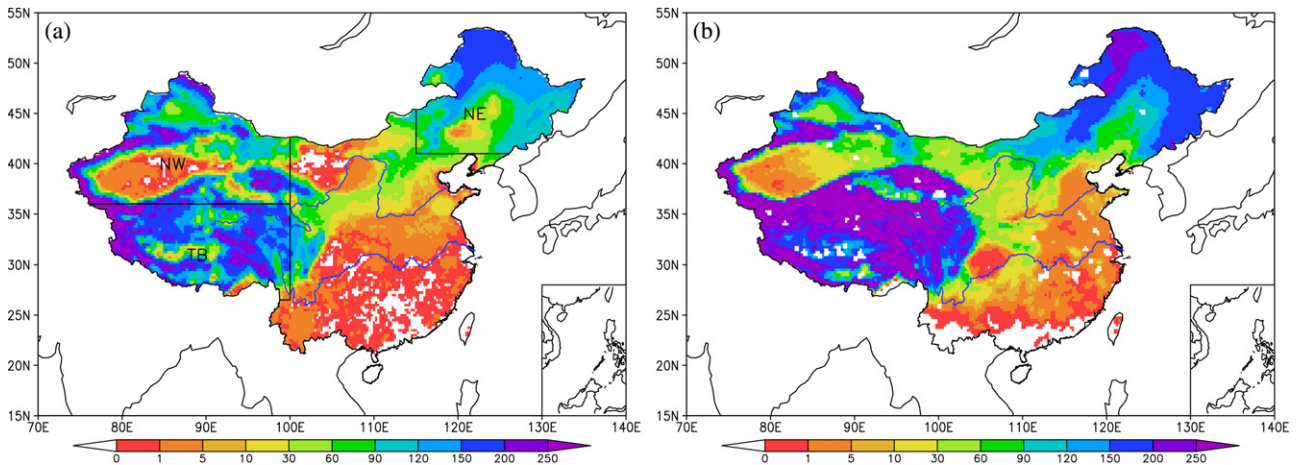
Figure 1. Observed (a) and simulated (b) annual mean number of SCDs over China (unit: days/year; the three sub-regions of NE, NW and TB in the study are shown in (a)).

substantially in winter despite the greater warming (Lemke *et al* 2007, Dye 2002).

The distribution of snow cover and its long-term trend have been documented by many researchers based on various kinds of observations over different regions in China, especially over the NW and Tibetan Plateau (TB) regions. For example, as reported by Qin *et al* (2006), snow cover in the past 47 years from 1951 to 1997 in western China shows a long-term variability characterized by a large interannual variation superimposed on a small increase trend. Estimates from the daily snow cover depth over the TB observations for the period of 1957–92 are found to be a general increase (Li 1996). Analysis of the observations from 17 stations in the Tianshan Mountains in the NW from 1959 to 2003 by Yang *et al* (2007) show an increase of the maximum snow depth in the past 45 years, a slight increase in the number of snow cover days and no clear changes in the starting and ending dates for it.

Snow cover is an integrated response to both temperature and precipitation and in general exhibits strong negative/positive correlation with air temperature/precipitation. The presence or absence of snow cover in much of western China is a function of precipitation availability rather than temperature. For example, although significant warming is found in the cold seasons in Xinjiang in NW, the increase in precipitation leads to an increase of snow cover over the area in recent decades (Ke *et al* 1997, Ding and Qin 2009, Cui *et al* 2005, Wei *et al* 2005).

As reported by the Fourth Assessment Report of the Intergovernmental Panel on Climate Change (IPCC 2007), a warming in the range of 1.1–6.4 °C is projected by the end of the 21st century (2090–99) relative to 1980–99. Studies on future changes of snow cover over China are important, both for better understanding the future climate and in impact and adaptation studies of the climate change. However, compared to the large efforts devoted to observational analysis, relatively few studies on the topic have been conducted so far over the region (Song *et al* 2008, Shi *et al* 2010, Sun *et al* 2010, Wang *et al* 2010, Ma *et al* 2011). Recently, a high resolution climate change simulation for the period of 1951–2100 was completed using a regional climate model at 25 km grid spacing (Gao *et al*

2011). Therefore we present an analysis of projected changes in snow cover over China in this paper based on this simulation.

The paper is organized as follows. Brief descriptions of the model and experiment design, as well as observation data and the definition of the terms used in the paper, are provided in section 2. This is followed by a basic validation of the model performance in simulating present snow cover in section 3. The projected changes are then analyzed in section 4, and section 5 presents our main conclusions.

2. The model, experiment design, data and method

The regional climate model employed in the experiment is the Abdus Salam International Centre for Theoretical Physics (ICTP) Regional Climate Model (RegCM3), which is an upgrade from the previous version RegCM2 (Pal *et al* 2007, Giorgi *et al* 1993a, 1993b). The model domain covers the whole of China and the surrounding areas with a grid spacing of 25 km. The simulation is conducted from 1948 to 2100 while the first three years are used as model spin-up and not included in the analysis. The observed greenhouse gas concentration for the present day simulation (before 2000) and the IPCC SRES A1B emission scenario (Nakicenovic 2000) for the future (after 2001) are used in the simulation. The initial and time evolving lateral boundary conditions are derived from the climate change simulations carried out using the global model of CCSR/NIES/FRCGC MIROC3.2_hires (K-1 Model Developers 2004). Snow depth in RegCM3 is prognostically calculated from snowfall, snowmelt, and sublimation. Precipitation is assumed to be in the form of snowfall if the temperature of the lowest model level is below -2 °C. Snow melting is calculated on the basis of the energy balance in the surface.

More detailed information on the model settings and experimental design can be found in Gao *et al* (2011). In Gao *et al* (2011), validation of the model performances in simulating the present temperature and precipitation are conducted, and their future changes are presented. They show a general warming in the future over China. The warming is more significant in the cold seasons and in the northern part of the
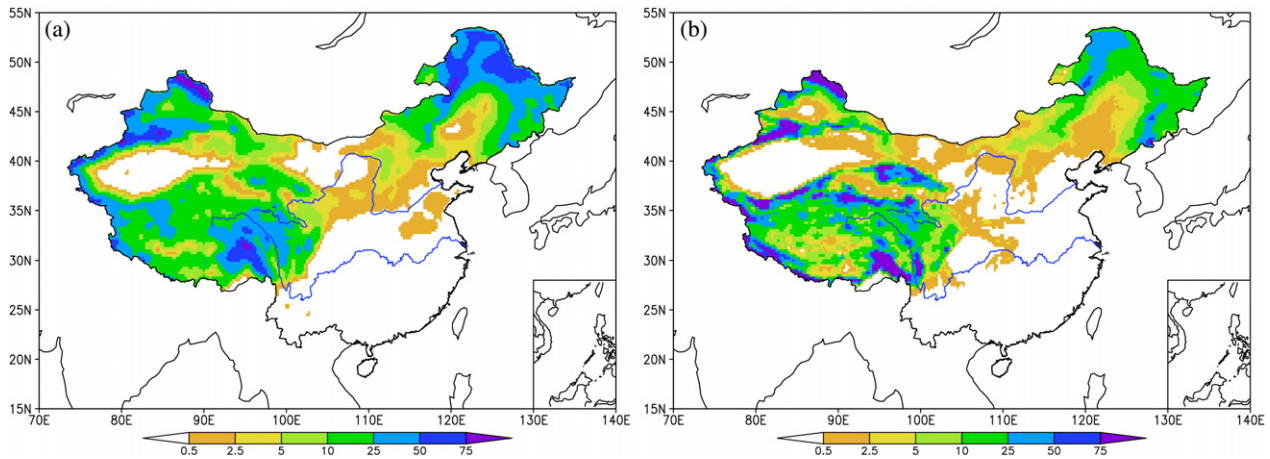
Figure 2. Annual mean snow depth from observation ((a) unit: mm) and simulation ((b) unit: mm SWE).

domain, as well as in the Tibetan Plateau. Increased/decreased precipitation over the north/south is simulated in winter, while in summer, there is an increase/decrease in Northwest China/Tibetan Plateau and a mixture of increase/decrease in eastern China are found. As was done in Gao *et al* (2011), we use 1981–2000 as the present day period, and 2001–2100 as the future simulation in the analysis.

The data set of snow depth in China developed by Che *et al* (2004) is employed to evaluate the model performances in the study. It is based on satellite remote sensing with calibration from station observations. The data set is daily, with a resolution of 25 km × 25 km. To facilitate the analysis, the data and the model output are bi-linearly interpolated to a common 0.25° × 0.25° grid size. The period 1981–2100 out of the 1978–2005 part of the data set is used to compare with the present day RegCM3 simulation. It is noted that the data set gives the depth of the snow while the model output gives the depth of the snow water equivalent (SWE). Thus, except as regards the spatial distribution, the comparison is more illustrative as concerns the 'depth' of the snow cover.

In the study, a snow cover day is defined as a day when the snow depth is deeper than 1 cm in the observation, and SWE greater than 1 mm in the simulation. The number of snow cover days (SCDs) is the total number of days with snow cover in an annual cycle of the snow (snow year), which starts from the first day of September and ends on the last day of the next August. The starting date of snow cover (SCSD) is defined as the date of the first snow cover day, and its ending date (SCED) as the last snow cover day in the snow year. SCED is always later than SCSD. SCSD and SCED are expressed as the cumulative number of days from 1 September, e.g. 31 indicates 1 October, 155 indicates 2 February, etc.

3. Validation of the present day simulation

3.1. Annual mean SCDs

Figure 1 displays the observed and simulated present day distributions of multi-annual mean SCDs over China. Values greater than 90 are found in both the high altitude and high latitude areas of TB, Northeast (NE) and NW from observation (figure 1(a)). In the plain areas north of the Yangtze River

in eastern China, the SCDs are mostly in the range of 1–30. Almost no snow cover can be found in most parts of the warm southern China (south of the Yangtze River), or in the desert area of Tarim Basin and the Junggar Basin in NW and Inner Mongolia. The SCDs in these areas are mostly less than 1, and even zero in some areas.

The simulated spatial distribution of SCDs is in general consistent with the observation, as shown in figure 1(b), and is also supported by a spatial correlation coefficient of 0.68 between the two. The areas with large numbers of SCDs can be found in TB, NE and NW as in the observation. The model also captures the fine scale features caused by small scale topography, such as the maxima over the Tianshan and Qilian Mountains and the minima or lower values over their adjacent areas (Tarim, Junggar and Qaidam Basins). Meanwhile, the model tends to overestimate the number of SCDs over the region. For example, over 10 SCDs are simulated over Hetao and the areas west to it in the simulation, instead of less than 1 as in the observation. Discrepancies of the model in simulating both temperature and precipitation can contribute to this overestimation—for example, the excessive precipitation simulated by the model in the winter season over these places (Gao *et al* 2011).

The areas with greater than 60 SCDs are usually considered as stable snow cover areas in China. They are the major containers of snow water resources and are the areas where many large rivers originate, especially in the west (Li and Mi 1983). As shown in figure 1(a), they are mainly located in NE and northern parts of NW and TB, which cover about 20% of China's land area. However, the simulated stable snow cover areas appear to be larger by a factor of 2 compared to those observed, due to the overestimation of SCDs. Note that those are the areas usually with few or no station observations available for calibrating the satellite data. Thus besides the model's deficiency, the lesser reliability and uncertainties of the 'observation' data used may also contribute to this discrepancy (Che *et al* 2004).

3.2. The annual mean snow cover amount

Figures 2(a) and (b) provide the observed and simulated annual mean snow cover depth. Comparison between the two
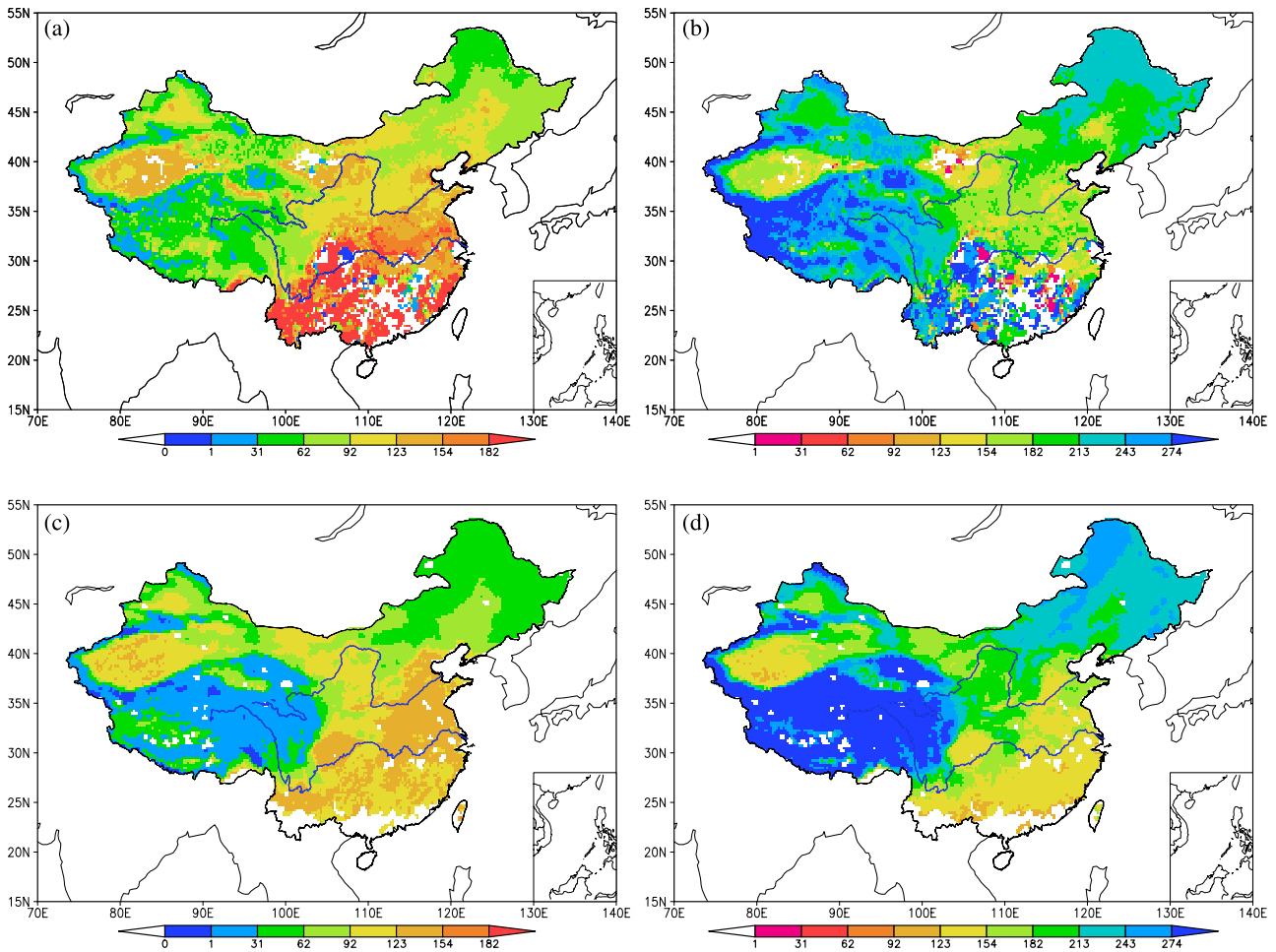
Figure 3. The SCSD and SCED from observation ((a), (b)) and simulation ((c), (d)); unit: days.

should be focused more on the relative amounts since they are in different units (mm and SWE, respectively). As can be found in the figure, the simulation basically reproduces the observed pattern of distribution. The three major snow cover areas of TB, NW and NE, and the barely snow covered areas of most parts of southern China, Tarim Basin, and Inner Mongolia are well described in the simulation. The model captures the features of the peak snow cover depth over the high mountains, e.g., Daxing'anling, Xiaoxing'anling, and Changbai Mountains in NE, and Tianshan and Altai Mountains in NW. The simulated relatively low values in the Qaidam Basin and the hinterland of TB also agree with the observation. The spatial correlation coefficient between the model simulation and observation is 0.21.

3.3. The annual mean SCSD and SCED

The observed and simulated SCSD and SCED are presented in figures 3(a)–(d), respectively. SCSD in the observation over eastern China shows a distinct latitudinal distribution (figure 3(a)). It increases from north to south, indicating a gradually later appearance of the snow cover down to the south. In western China, SCSD shows a strong dependence on the topography, with smaller values and earlier dates found over

the high peaks. In general, the values in excess of 150 are found in most parts of southern China, corresponding to a first appearance of snow cover only after February. Areas with no snow cover in the multi-annual mean are found in portions in southern China, as well as in the Tarim Basin and Inner Mongolia in the north. Lower values corresponding to a very early appearance in October or even September can be found in NE, Tianshan and the Altai Mountains, and most parts of TB.

The simulated distribution of SCSD (figure 3(b)) in general agrees with observation both in eastern and western China. However the areas where the conditions do not satisfy the SCSD criteria are less than in the observation, and mainly located in areas south of 25°N. Furthermore, most of the simulated SCSD are earlier than in the observation, mostly due to the overestimation of precipitation in winter over the region (Gao *et al* 2011). The small portions of areas with very much earlier SCSD in southern China are considered as random errors in the observation data (see figures 1(a) and 3(c)) because of their very short lifetime.

The SCED are mostly greater than 150 in the observation (figure 3(c)) over the region, except in southern China. Like SCSD, it also follows the latitudinal distribution in the east, and topographic dependence in the west. Greater values of SCED are found in the three major snow cover areas of NW,
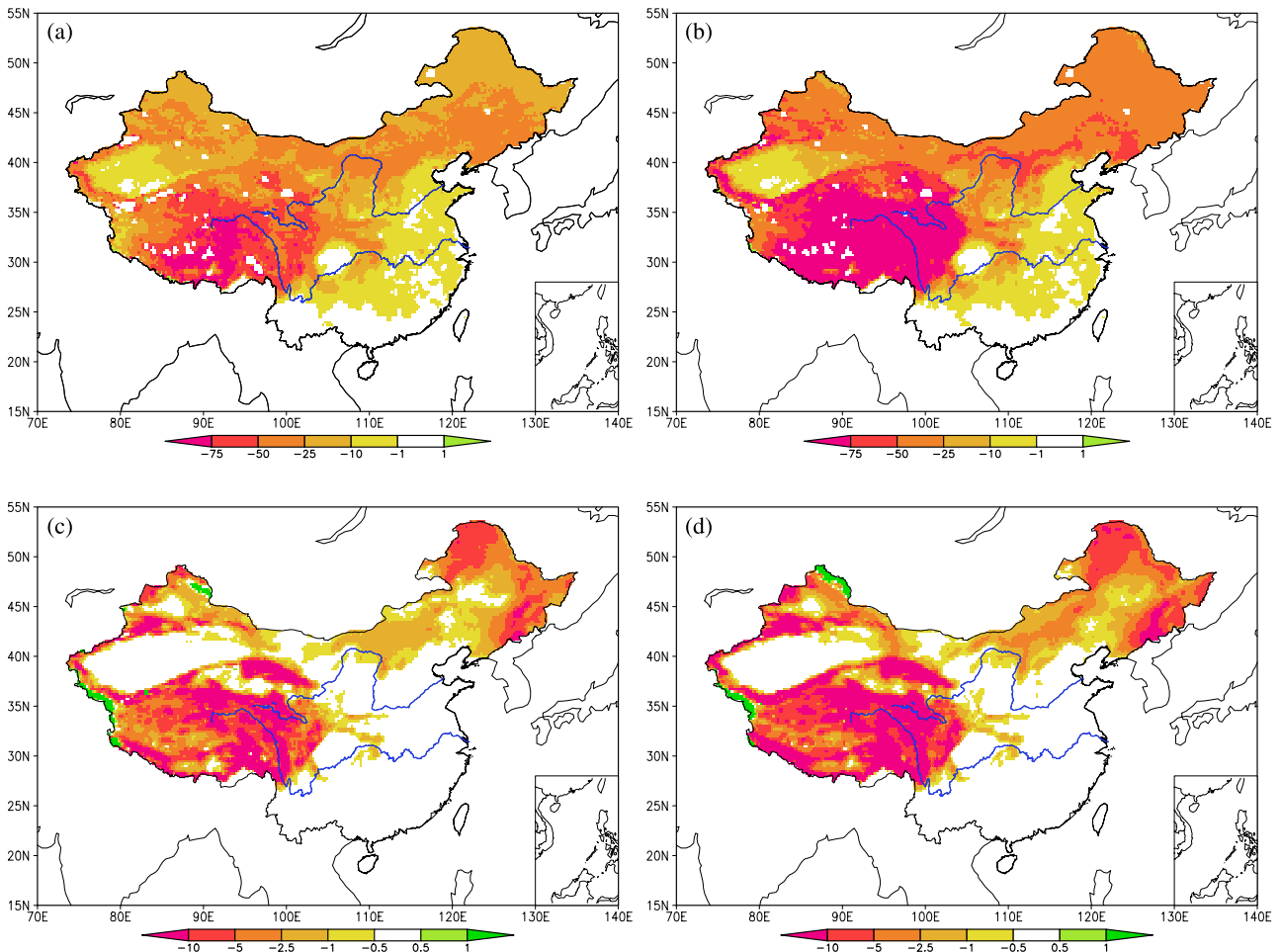
Figure 4. Changes of annual mean SCDs ((a), (b)) and snow cover depth ((c), (d)) over China by the middle and end of the 21st century (units: days/year and mm SWE).

NE and TB, with the maxima located at the mountain peaks in NW and TB. The simulated SCED (figure 3(d)) are also consistent with the observation both in the general pattern and the spatial details, e.g. the earlier SCED in Qaidam Basin and the hinterland of TB, and the later SCED in Tianshan and the Qilian Mountains compared to the surrounding areas. Like for SCSD, generally later SCED are found in the simulation compared with the observation in most of the areas. The spatial coefficients of correlation between the simulations and observations for SCSD and SCED are 0.43 and 0.38, respectively.

4. Future changes

### 4.1. Changes of SCDs and snow cover depth

The 150 year continuous simulation in the study includes 149 snow years. Of the total 149 years, the period 2041–60 is selected as the middle of the 21st century and 2081–99 as the end of the century. Firstly, changes of SCDs in the middle and end of the 21st century are presented in figures 4(a) and (b) respectively. Overall decreases of SCDs can be found in both time periods, with larger magnitude in the later one. Greater decrease is simulated over NE, NW and TB while

the decrease is most pronounced in TB, with the values in excess of 50 and 75 in the middle and end of the 21st century. This notable decrease in TB is closely related to the simulated significant reduction of precipitation there (Gao *et al* 2011). Note that greater warming can be found over those areas with greater decrease of SCDs, which can be largely explained by the positive feedback between the decreased surface albedo associated with the melting of snow and the warming (Giorgi *et al* 1997).

The simulated snow cover depths in both periods are also found to show a dominant decrease over the region, except for a slight increase in some places in NW and TB (figures 4(c) and (d)). The maximum decrease of snow cover depth is larger than 10 mm SWE in both the middle and end of the 21st century, with a larger spread for the later period. Unlike for SCDs, the decrease is more pronounced in the mountainous areas in NW and NE, corresponding to the larger value of the snow cover depth there in the present day (see figure 2(b)).

4.2. Changes in SCSD and SCED

Figure 5 illustrates changes of SCSD and SCED in the middle and end of the 21st century. As can be observed from figure 5(a), SCSD is simulated in general to be delayed in
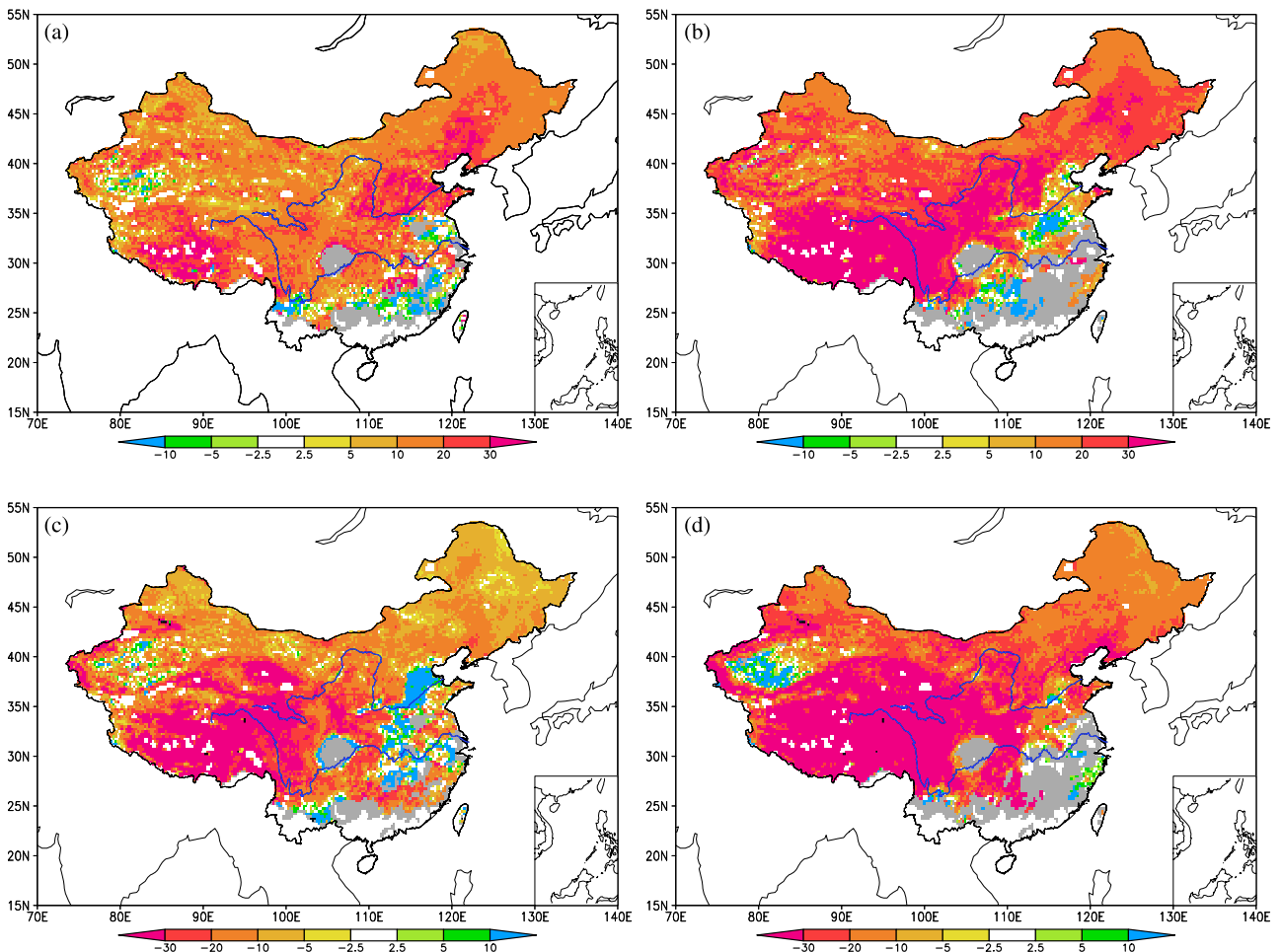
Figure 5. Changes of SCSD ((a), (b)) and SCED ((c), (d)) by the middle and end of the 21st century (unit: days); gray indicates areas that meet the condition of SCSD or SCED in the present day but not in the future.

the middle of the 21st century, which is in line with the common understanding of it under global warming. The delay is mostly less than 20 days whereas in the central part of TB, southern parts of NE and North China, it can be up to 30. Instead, an earlier SCSD over 10 days is found in portions of southern China, Huanghuai area, and parts of the Tarim Basin. The changes of SCSD in the end of the 21st century (figure 5(b)) show a pattern similar to that in the middle, but more pronounced. Delays of SCSD over 30 days can be found widely in TB, and the areas northeast of it. Areas with earlier SCSD can still be found in the end of the century, although the locations are slightly different from those in the middle. More areas where the condition of SCSD is satisfied in the present day but not in the future are simulated, indicating the expansion of snow cover free areas in the end of the century.

SCED are simulated to be 5–30 days earlier in most of the areas with the maxima greater than 30 days located in TB and the Qilian Mountains in the middle of the 21st century (figure 5(c)). In contrast to the generally earlier SCED, a postponement over 10 days is found in the plain areas of North China, along the Yangtze River and portions of the Tarim Basin. A similar change pattern of SCED but further advanced can be found in the end of the 21st century (figure 5(d)). The

spread of delayed SCED becomes narrower in eastern China, but wider in the Tarim Basin.

Changes in SCDs and the snow cover depth, as well as SCSD and SCED, are the results of a combination of changes in both temperature and precipitation. As water vapor in the air increases due to the warming, precipitation in the form of snowfall may increase over some regions, leading to an earlier or later snow cover in the future. This is also simulated by other models over other regions (Christensen *et al* 2007).

4.3. Sub-regional mean changes over NE, NW and TB

Mean changes of SCDs, the snow cover depth, SCSD and SCED over the three sub-regions of TB, NE and NW as shown in figure 1(a) in the 21st century are presented in figures 6(a)–(d), respectively. Decreases of SCDs are found over all of the three sub-regions in the 21st century (figure 6(a)). The decrease is relatively weak in NE and NW, and more pronounced in TB. The linear trends of the decrease during 2021–99 over the three sub-regions are 3, 4, and 11 days/decade, respectively. Similar decreases of the snow cover depth can be found in figure 6(b), with the linear trends of 0.3, 0.6 and 1.5 mm SWE/decade over the three sub-regions.
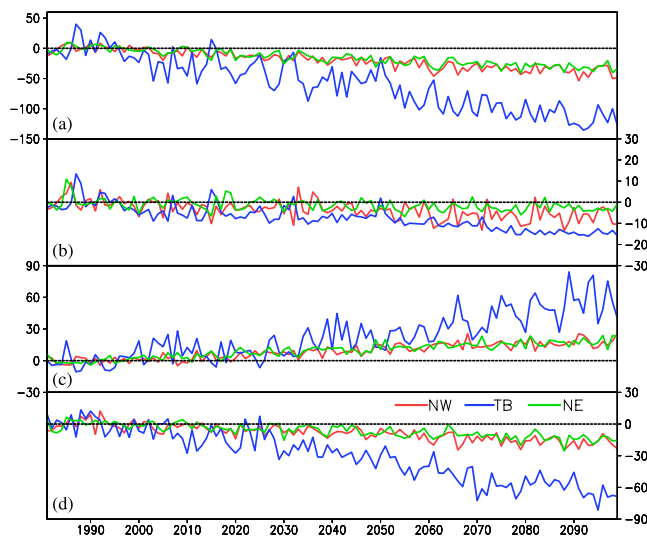
Figure 6. Mean changes (anomalies) of SCDs ((a) unit: days/year), the snow cover depth ((b) unit: mm SWE), SCSD ((c) unit: days) and SCED ((d) unit: days) over the three sub-regions during 1981–2099 (red—NW, blue—TB, green—NE).

Changes in SCSD show a stepwise delay in the future. The trends in NE and NW are close to each other with the value around 1 day/decade during 2021–99, while a much stronger trend of 6 day/decade is simulated over TB. Advanced SCED over the three sub-regions are found (figure 6(d)), corresponding to the reduction of snow cover days and snowfall in the future. The trends for SCED in NE and NW are still close to each other, with the values being 1 and 2 day/decade, respectively. The trend is much larger in TB, and reaches 7 day/decade, where the SCED changes from 320 in the present day to 260 by the end of the 21st century.

5. Conclusions and discussion

Snow cover and its changes are closely related to temperature and precipitation, and vary with elevation and latitudes. The overall diverse climate over China adds to the difficulties in the topic. As an integrated tool which considers and includes most of the factors and processes, application of the high resolution climate model is important in addressing the vexing issues of snow cover and its changes. In this study, on the basis of simulations conducted using RegCM3 at 25 km grid spacing, we analyze the changes in snow cover over China in the 21st century. The analysis includes SCDs, the snow cover depth, SCSD and SCED. It starts with the comparison between the limited available observations and simulations for evaluating the model performances. Then the future changes are presented. Our main results can be summarized as follows.

The model is generally successful in reproducing the principal features of SCDs, the snow cover depth, SCSD and SCED in the present day as regards the spatial distributions. But discrepancies exist in simulating their amounts. Overestimation of SCDs, earlier SCSD and later SCED are simulated, which may be primarily due to the excessive precipitation (snowfall) in the cold seasons in the model simulations.

Climate warming in the future also leads to significant changes in snow cover. In general, fewer SCDs and reduced snow cover depth can be found in most areas over China. The changes become larger over time in the 21st century, with the most profound changes located in TB. SCSD is simulated to be delayed while SCED is simulated to be advanced in most areas, as expected under the warming. However areas with the changes in the opposite direction can be found. For example, the SCSD becomes earlier in southern China while the SCED becomes later in the north of China in the middle of the 21st century.

Due to the data availability, satellite remote sensing based data are employed in the study in validating the model performances. It is noted that there are over 2400 weather stations across China managed by China Meteorological Administration and over 1000 additional stations under other departments (e.g., hydrology, forestry, agriculture, etc). Collection of the snowfall and snow cover data from those observation stations, and interpolating them into a higher resolution gridded data set (Xu *et al* 2009), will provide great help in model validation and development, and is planned for future work.

As mentioned above, the deficiencies of the model in simulating either temperature or precipitation can lead to errors in the projected snow changes. The performances of the model show differences over different areas of China. Furthermore, the consideration of snow cover in the land surface scheme in RegCM3 is rather simple. Improvements of the model are indeed needed in future work to add to the robustness of the results.

Finally, in one of the few high resolution regional climate simulations available so far over the region, Shi *et al* (2010) reported the changes of snow cover in the end of the 21st century as simulated using the same regional climate model but driven by a different global model (FvGCM) under the A2 scenario. Consistencies can be found in the general decrease of SCDs and snow cover depth, as well as the postponed SCSD and advanced SCED. Areas with advanced SCSD and postponed SCED were also reported, but in different locations. In addition, increases of SCDs and snow cover depth were found in the simulations by Shi *et al* (2010). This emphasizes the requirements of conducting multi-model ensemble simulations in the future in order to better address and reduce the uncertainties concerning the snow cover changes over China (Giorgi *et al* 2009).

Acknowledgments

References

Che T *et al* 2004 Estimation of snow water equivalent in the Tibetan Plateau using passive microwave remote sensing data *J. Glaciol. Geocryol.* **26** 363–8

Chen L T 2001 The role of the anomalous snow cover over the Qinghai-Xizang plateau and ENSO in the great floods of 1998 in the Changjiang river valley *Chin. J. Atmos. Sci.* **25** 184–92

Christensen J H *et al* 2007 Regional climate projections *Climate Change 2007: The Physical Science Basis. Contribution of Working Group 1 to the Fourth Assessment Report of the Intergovernmental Panel on Climate Change* ed S Solomon *et al* (Cambridge: Cambridge University Press)

Cui C X *et al* 2005 Comparison analysis of the long-term variations of snow cover between mountain and plain areas in Xinjiang region from 1960 to 2003 *J. Glaciol. Geocryol.* **27** 486–90

Ding Y J and Qin D H 2009 Cryosphere change and global warming: impact and challenges in China *China Basic Sci.* **3** 4–10

Dye D G 2002 Variability and trends in the annual snow-cover cycle in Northern Hemisphere land areas, 1972–2000 *Hydrol. Process.* **16** 3065–77

Gao X J *et al* 2011 A high resolution climate change simulation of the 21st century over China by RegCM3 *Chinese Sci. Bull.* submitted

Giorgi F *et al* 1993a Development of a second-generation regional climate model (RegCM2). Part I: boundary-layer and radiative transfer processes *Mon. Weather Rev.* **121** 2794–813

Giorgi F *et al* 1993b Development of a second-generation regional climate model (RegCM2). Part II: convective processes and assimilation of lateral boundary conditions *Mon. Weather Rev.* **121** 2814–32

Giorgi F *et al* 1997 Elevation signal in surface climate change: a model study *J. Clim.* **10** 288–96

Giorgi F *et al* 2009 Addressing climate information needs at the regional level: the CORDEX framework *WMO Bull.* **58** 175–83

Hasumi H and Emori S (ed) 2004 K-1 Model Developers *K-1 Coupled Model (MIROC) Description. K-1 Technical Report 1* (Tokyo: Center for Climate System Research, University of Tokyo) p 34 (www.ccsr.u-tokyo.ac.jp/kyosei/hasumi/MIROC/tech-repo.pdf)

IPCC 2007 *Climate Change 2007: The Physical Science Basis. Contribution of Working Group 1 to the Fourth Assessment Report of the Intergovernmental Panel on Climate Change* ed S Solomon *et al* (Cambridge: Cambridge University Press) p 996

Ke C Q *et al* 1997 Variation trends of snow cover over the Tibetan Plateau and their relations to temperature and precipitation *J. Glaciol. Geocryol.* **19** 289–94

Lemke P *et al* 2007 Observations: changes in snow, ice and frozen ground *Climate Change 2007: The Physical Science Basis. Contribution of Working Group 1 to the Fourth Assessment Report of the Intergovernmental Panel on Climate Change* ed S Solomon *et al* (Cambridge: Cambridge University Press)

Li P J 1996 Response of Tibetan snow cover to global warming *Acta Geogr. Sin.* **51** 260–5

Li P J and Mi D S 1983 Distribution of snow cover in China *J. Glaciol. Geocryol.* **5** 9–17

Ma L J *et al* 2011 Snow water equivalent over Eurasia in the next 50 years projected by CMIP3 models *J. Glaciol. Geocryol.* **33** 707–20

Nakicenovic N *et al* 2000 *IPCC, Special Report on Emissions Scenarios* (New York: Cambridge University Press) pp 1–599

Pal J S *et al* 2007 Regional climate modeling for the developing world: the ICTP RegCM3 and RegCNET *Bull. Am. Meteorol. Soc.* **88** 1395–409

Qin D H *et al* 2006 Snow cover distribution, variability, and response to climate change in western China *J. Clim.* **19** 1820–33

Shi Y *et al* 2010 Simulation of the changes in snow cover over China under global warming by a high resolution RCM *J. Glaciol. Geocryol.* **32** 215–22

Song R Y *et al* 2008 Simulation of changes in cold events in southern China under global warming *Adv. Clim. Change Res.* **4** 352–6

Sun J Q *et al* 2010 Spatial–temporal features of intense snowfall events in China and their possible change *J. Geophys. Res.* **115** D16110

Wang C H *et al* 2010 A prediction of snow cover depth in the Northern Xinjiang in the next 50 years *J. Glaciol. Geocryol.* **32** 1059–65

Wei Z G *et al* 2005 The causes of the interannual variation of snow cover over the Tibetan Plateau *J. Glaciol. Geocryol.* **27** 491–7

Xu Y *et al* 2009 A daily temperature dataset over China and its application in validating a RCM simulation *Adv. Atmos. Sci.* **26** 763–72

Yang Q *et al* 2007 Snow cover variation during 1959–2003 in Tianshan mountains China *Adv. Clim. Change Res.* **3** 80–4